Continuum-discretized coupled-channels study of the ^{11}Be$\rightarrow$ ^{10}Be$+n$ breakup effect on ^{11}Be elastic scattering

M. Takashina,* S. Takagi, and Y. Sakuragi
Department of Physics, Osaka City University, Osaka 558-8585, Japan

Y. Iseri
Department of Physics, Chiba-Keizai College, Chiba 263-0021, Japan
(Received 30 November 2002; published 14 March 2003)

The ^{11}Be$\rightarrow$ ^{10}Be$+n$ breakup effect on the elastic scattering of ^{11}Be by ^{12}C at $E/A=49.3$ MeV is investigated by the method of continuum-discretized coupled-channels (CDCC) based on the ^{10}Be$+n+$target three-body model. The CDCC calculation well reproduces the experimental data of the elastic scattering, which is consistent with the result of recent studies based on the adiabatic three-body models. The breakup effect is significant and the coupling to the *p*-wave continuum states and the *d*-wave resonance state have a dominant contribution to the breakup effect. Dynamical polarization potential which simulates the breakup effect is evaluated and found to have a weakly repulsive real part and a long-range imaginary part of absorptive nature, characteristic of the weakly bound projectile with neutron halo.

DOI: 10.1103/PhysRevC.67.037601 PACS number(s): 24.10.Eq, 25.60.Bx

Nuclear reactions involving neutron-rich nuclei have been one of the most important subjects in nuclear physics. Particularly, recent nuclear-reaction data with light neutron-halo nuclei provide us with fruitful information to test existing nuclear-reaction theories and promote us to invent new techniques and models applicable to the study of such new types of experimental data.

A new adiabatic three-body model recently proposed by Johnson *et al.* [1] provides us with a very simple method of solving a complicated three-body problem based on the adiabatic approximation. This model incorporates the weakly bound nature of a neutron-halo nucleus consisting of a relatively heavy core nucleus plus a single halo neutron. Namely, it freezes up the internal motion of the halo neutron in the projectile nucleus (adiabatic approximation) and neglects the interaction between the halo neutron and the target nucleus, which is expected to be weak compared with the interaction between the core nucleus and the target. This model was first applied to the elastic scattering of a neutron-halo nucleus ^{11}Be on the ^{12}C target at $E/A=49.3$ MeV and subsequently to the Coulomb-breakup reactions of halo nuclei and deuterons on heavy target nuclei. In the application to elastic scattering, the calculated result by this new model was compared with that of the full adiabatic-model calculation, in which the adiabatic three-body equation [2] was solved exactly without neglecting the interaction between the halo neutron and the target nucleus. Although the *n*-target interaction had non-negligible effect, these two calculations gave similar results, both indicating a significant breakup effect of the ^{11}Be projectile.

The adiabatic approximation may be reasonable for elastic scattering at a high incident energy, which enables us to probe the ground state properties of the halo nucleus. However, in this approximation, we cannot pursue the details of reaction processes, because the projectile excitations including the breakup are not treated explicitly. In order to understand the reaction mechanism, it is very important to investigate the dynamical breakup process more explicitly, that is, which part of the breakup state in ^{11}Be has a dominant effect on the elastic scattering. Furthermore, it is interesting to investigate how the halo structure affects the reaction mechanisms. Therefore, in order to study the dynamical breakup effect on the halo-nucleus induced reaction in detail, one needs to solve the three-body problem by a nonadiabatic framework.

One of the practical and reliable nonadiabatic methods to study the three-body reaction process is the continuum-discretized coupled-channels (CDCC) method [3,4]. In the CDCC method, the continuum-energy two-body breakup states of the projectile nucleus are approximately represented in terms of a finite number of discretized states in the prescription called the method of momentum bins. The discretized breakup states can be treated in the same manner as usual discrete excited states and coupled-channels equations are numerically solved in the standard way to obtain the transition matrix elements for elastic scattering and breakup reactions. In the present paper, we apply the CDCC method to study the ^{11}Be$\rightarrow$ ^{10}Be$+n$ breakup effect on the elastic scattering of ^{11}Be by ^{12}C at $E/A=49.3$ MeV and investigate the reaction mechanism induced by the halo nucleus.

Since the separation energy of ^{11}Be into ^{10}Be and *n* is small, the ^{11}Be breakup reaction takes place mainly as a binary projectile-breakup process ^{11}Be into ^{10}Be$+n$. In the present study, wave functions describing the relative motion between ^{10}Be and *n* are calculated with a Woods-Saxon type potential of geometry $R_0=1.00\times A_c^{1/3}$ fm with $A_c=10$ and $a_0=0.53$ fm, which is the same as that used in Ref. [5]. The depth of the potential V_0 is adjusted to reproduce the separation energies E_s of the ground state ($2s$, $E_s=0.503$ MeV) for the *s* wave ($\ell=0$, where ℓ represents the orbital angular momentum of *n* relative to the ^{10}Be core), the first excited

*Electronic address: takasina@ocunp.hep.osaka-cu.ac.jp

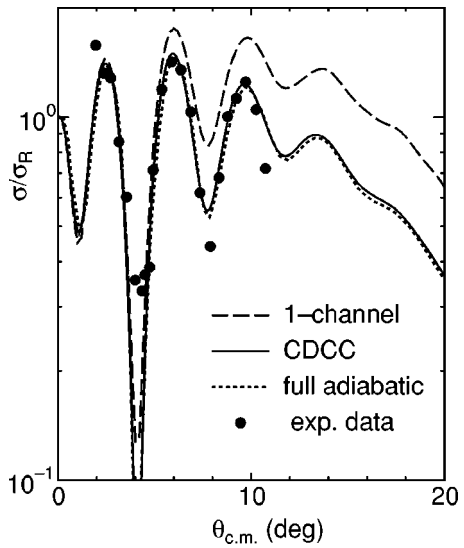

FIG. 1. Angular distribution for the ^{11}Be+ ^{12}C elastic scattering at $E/A=49.3$ MeV. The dashed and solid curves represent the results of the single-channel and CDCC calculations, and the dotted curve represents the result of the full adiabatic calculation. The filled circles are the experimental data.

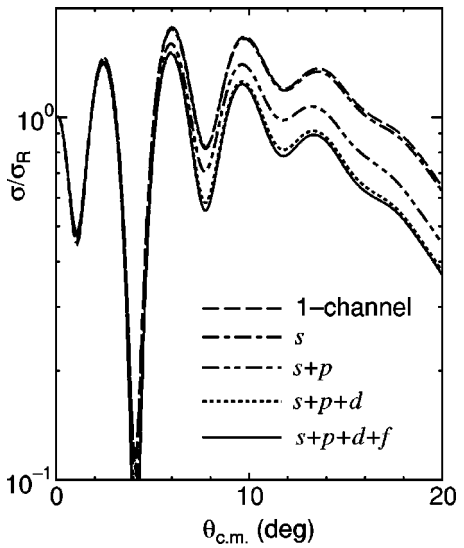

FIG. 2. The results of the single-channel calculation (dashed), and of the CDCC calculations including the breakup states up to s (dot-dashed), p (double-dot-dashed), d (dotted), and f waves (solid).

state $(1p,E_s=0.183$ MeV) for the p wave $(\ell=1)$, and the resonance energy $(E_r=1.275$ MeV) for the d wave $(\ell=2)$, respectively. For the odd and even partial waves greater than $\ell=2$, we use the same values of V_0 as those for the p and d waves, respectively. The spin-orbit interaction is neglected for simplicity.

In the CDCC method [3,4], the continuum state in ^{11}Be above the ^{10}Be$+n$ breakup threshold $E_x>0.503$ MeV is truncated in k space at $k_{\max}$ and discretized into momentum bins of width Δk, where k denotes the linear momentum of the ^{10}Be$+n$ relative motion. The values of $k_{\max}$ and Δk are determined so that the calculated S-matrix elements of the ^{11}Be+ ^{12}C elastic scattering converge with respect to the increase of $k_{\max}$ and to the decrease of Δk, respectively.

The discretized wave function in the ith bin is written as

$$\hat{\psi}_i(\mathbf{r})=\frac{1}{\sqrt{N_i}}\int_{\Delta k_i}\psi(\mathbf{r};k)f_i(k)dk, \tag{1}$$

where $1/\sqrt{N_i}$ is the normalization factor and $\mathbf{r}$ is the relative coordinate between ^{10}Be and n. $f_i(k)$ represents the weight function, the form of which is the same as that used in Ref. [4], namely $f_i(k)=1$ for nonresonance bins and Lorentzian form is used for resonance bins.

In terms of the discretized wave functions Eq. (1) as well as the bound-state wave functions, the interaction U_{ij} between ^{11}Be and ^{12}C is calculated by the cluster-folding model. The diagonal $(i=j)$ or coupling $(i\neq j)$ nuclear potential is written as

$$U_{ij}(\mathbf{R})=\left\langle \hat{\psi}_i(\mathbf{r})\left| U_v\left(\left|\mathbf{R}-\frac{10}{11}\mathbf{r}\right|\right)+U_c\left(\left|\mathbf{R}+\frac{1}{11}\mathbf{r}\right|\right)\right|\hat{\psi}_j(\mathbf{r})\right\rangle, \tag{2}$$

where $\mathbf{R}$ represents the relative coordinate between ^{11}Be and ^{12}C. U_v and U_c represent the optical potential between n and ^{12}C, and that between ^{10}Be and ^{12}C, respectively. The potential parameters are given by the Becchetti-Greenlees parametrization [6] for U_v, while those for the latter are taken from Ref. [5]. The parameters for U_v are $V=37.4$ MeV, $r_0=1.20$ fm, $a_0=0.75$ fm, $W=10.0$ MeV, $r_I=1.30$ fm, $a_I=0.60$ fm, where the range parameters are multiplied by a factor of $12^{1/3}$, and those for U_c are $V=123.0$ MeV, $r_0=0.75$ fm, $a_0=0.80$ fm, $W=65.0$ MeV, $r_I=0.78$ fm, $a_I=0.80$ fm, where the range parameters are multiplied by a factor of $10^{1/3}+12^{1/3}$.

In the present study, Coulomb breakup is neglected and the Coulomb potential between ^{11}Be and ^{12}C is approximated by usual uniform-charge Coulomb potential with the charge-radius $R_c=1.2\times(10^{1/3}+12^{1/3})$ fm. The neglect of the Coulomb-breakup contribution is justified for the elastic scattering of this light system at the high energy.

The convergence of the S-matrix elements for the ^{11}Be $+$ ^{12}C elastic scattering is obtained when we take $k_{\max}=1.2$ fm^{-1}, and $\Delta k=0.133$ fm^{-1} for all the partial waves, except for the d wave, for which we take $\Delta k=0.157$ fm^{-1} for the lowest two bins and $\Delta k=0.127$ fm^{-1} for the other higher bins due to the existence of the resonance state. The differential cross section is sufficiently converged when we take into account the orbital angular momentum up to the f wave $(\ell=3)$.

Figure 1 shows the angular distribution of the ^{11}Be $+$ ^{12}C elastic scattering at $E/A=49.3$ MeV. The dashed curve shows the result of single-channel calculation using the cluster-folded potential Eq. (2), while the solid curve shows the result of the CDCC calculation. It is found that the breakup effect of ^{11}Be into ^{10}Be$+n$ is significant and largely reduces the cross section. The filled circles are the experimental data [1], which are found to be well reproduced by the present CDCC calculation. The dotted curve is the result of the full adiabatic calculation taken from Ref. [1], which is

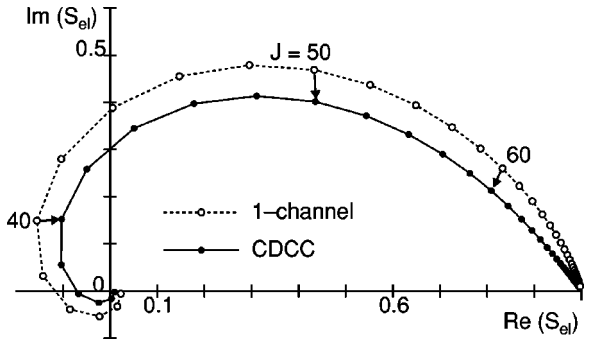

FIG. 3. The *S*-matrix elements for the elastic scattering of ^{11}Be from ^{12}C. The open circles with dotted curve and the solid circles with solid curve are for the single-channel and CDCC calculations, respectively.

close to that of the present CDCC calculation, indicating the validity of the adiabatic approximation at this energy.

Figure 2 shows the contributions of individual breakup states with different ℓ values. The solid and dashed curves are the same as those shown in Fig. 1. The dot-dashed, double-dot-dashed, and dotted curves represent the results of CDCC calculations including the breakup states up to the *s*, *p*, and *d* waves, respectively. The bound excited state in the *p* wave is also included, when the *p*-wave breakup states are included. The results indicate that the breakup effect is dominated by the coupling to the *p*- and *d*-wave breakup states, which play a very important role to reproduce the experimental data. It is also found that, among the *p*-wave breakup states, the second ($\hat{E}_x = 0.954$ MeV, where $\hat{E}_x$ represents the mean energy of the bin) and third ($\hat{E}_x = 2.592$ MeV) bins have the largest contribution, while, in the *d* wave, the bin containing the resonance state at $E_x = 1.778$ MeV has the largest contribution. The large contribution from the *p*-wave breakup states is a notable property characteristic to the halo nucleus. This can be understood as follows by a detailed analysis of the relation between the neutron wave functions in ^{11}Be and the breakup coupling matrix elements. Because of the halo nature of the ground state, the wave function of the *s*-wave neutron in the ground state is found to have a very large coupling matrix elements with those of the *p*-wave neutron in the breakup states, especially those in the second and third bins. The *d*-wave resonance state also has a fairly large coupling matrix element with the ground state.

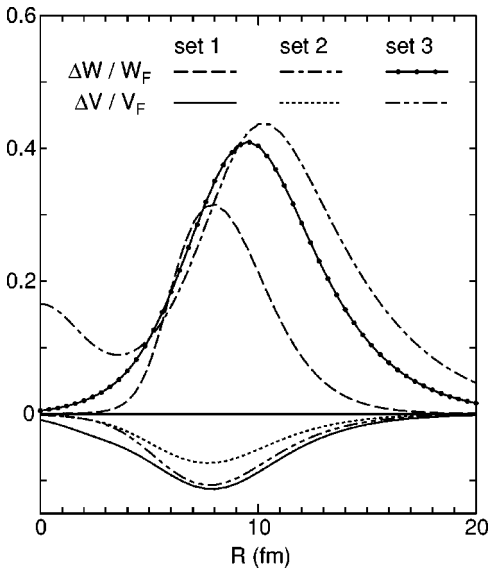

FIG. 4. Ratio of the dynamical polarization potential to the folded elastic potential. The results for three sets of the potential are shown.

In order to see the nature of the breakup effect on elastic scattering, we plot the *S*-matrix elements for individual partial waves of the elastic scattering in the complex *S* plane. In Fig. 3, the open circles with dotted curve represent the *S*-matrix elements of the single-channel calculation, while the solid circles with solid curve represent those of the CDCC calculation. It is clearly seen that the inclusion of the coupling rotates the *S*-matrix elements clockwise and reduces the absolute values of them, implying that the breakup effect is of a repulsive and an absorptive nature.

In order to see the breakup effect of ^{11}Be shown in Fig. 3 in the potential form, we evaluate the dynamical polarization potential (DPP) in the same manner as that used in Ref. [7]. We search effective potential of the form $U_{\rm eff} = U_F + \Delta U$, which reproduces the result of the CDCC calculation in the single-channel framework and, consequently, simulates the breakup effect. Here, U_F denotes the folded potential given by Eq. (2) for the elastic channel, while we assume the Woods-Saxon derivative form for both the real (ΔV) and imaginary (ΔW) parts of ΔU. For the potential search process we use the computer code ALPS [8].

We find three parameter sets for ΔU which fit the result of the CDCC calculation. It should be noted that the *S*-matrix

TABLE I. Parameter sets of the dynamical polarization potential.

Set	Real (ΔV) [a]			Imaginary (ΔW) [a]		
	V_D (MeV)	r_V (fm) [b]	a_V (fm)	W_D (MeV)	r_W (fm) [b]	a_W (fm)
set 1	3.302	1.099	1.140	-0.718	2.293	0.894
set 2	1.182	1.493	1.092	-10.90	0.002	1.364
set 3	1.372	1.597	1.095	-1.584	1.495	1.202

[a]Defined as $\Delta V(R) = 4V_D \exp[(R-R_V)/a_V]/\{1+\exp[(R-R_V)/a_V]\}^2$ and $\Delta W(R) = 4W_D \exp[(R-R_W)/a_W]/\{1+\exp[(R-R_W)/a_W]\}^2$.

[b]$R_x = r_x A_T^{1/3}$ for $x = V$ or W, where $A_T = 12$.

elements with $U_{\rm eff}$ are indeed close to the elastic-channel *S*-matrix elements of the CDCC calculation. The potential parameters are given in Table I, and the polarization potential evaluated as ratio to the folded potential is shown in Fig. 4. It is found that the real part of all the three DPP's is found to have opposite sign of U_F (repulsive) and to reduce the real part of the effective potential $U_{\rm eff}$ by about 10% at $r \approx 7.5$ fm where the elastic scattering is the most sensitive to the potential. On the other hand, the imaginary part of DPP's has the same sign as that of the folded potential U_F (absorptive) and is of longer range than the real part [9]. Its strength amounts to about 30% of the imaginary part of U_F in this region. This result reflects the characteristic of the weakly bound halo structure of the ^{11}Be nucleus.

[1] R.C. Johnson, J.S. Al-Khalili, and J.A. Tostevin, Phys. Rev. Lett. **79**, 2771 (1997).
[2] H. Amakawa, S. Yamaji, A. Mori, and K. Yazaki, Phys. Lett. **82B**, 13 (1979).
[3] N. Austern, Y. Iseri, M. Kamimura, M. Kawai, G.H. Rawitscher, and M. Yahiro, Phys. Rep. **154**, 125 (1987).
[4] Y. Sakuragi, M. Yahiro, and M. Kamimura, Prog. Theor. Phys. Suppl. **89**, 136 (1986).
[5] J.S. Al-Khalili, J.A. Tostevin, and J.M. Brooke, Phys. Rev. C **55**, R1018 (1997).
[6] F.D. Becchetti and G.W. Greenlees, Phys. Rev. **182**, 1190 (1969).
[7] Y. Hirabayashi, S. Okabe, and Y. Sakuragi, Phys. Lett. B **221**, 227 (1989).
[8] Y. Iseri, computer code ALPS (unpublished).
[9] J.S. Al-Khalili and J.A. Tostevin, Phys. Rev. C **49**, 386 (1994).